A novel passive micromixer based on unbalanced splits and collisions of fluid streams

2010 J. Micromech. Microeng. 20 055007

(http://iopscience.iop.org/0960-1317/20/5/055007)

J. Micromech. Microeng. **20** (2010) 055007 (10pp) doi:10.1088/0960-1317/20/5/055007

A novel passive micromixer based on unbalanced splits and collisions of fluid streams

Mubashshir Ahmad Ansari, Kwang-Yong Kim[1], Khalid Anwar and Sun Min Kim

Department of Mechanical Engineering, Inha University, 253 Younghyun-dong, Nam-gu, Incheon, 402-751, Korea

E-mail: kykim@inha.ac.kr

Received 17 November 2009, in final form 22 February 2010
Published 7 April 2010
Online at stacks.iop.org/JMM/20/055007

Abstract

A new passive micromixer based on the concept of unbalanced splits and cross-collisions of fluid streams is designed and fabricated. Experimental and numerical studies have been carried out on the micromixer at Reynolds numbers ranging from 10 to 80. The three-dimensional Navier–Stokes equations have been used to analyze the mixing and flow behavior of the micromixer, which is composed of two sub-channels of unequal widths which repeatedly undergo splitting and recombination. The difference between the mass flow rates in the two sub-channels creates an unbalanced collision of the two fluid streams. Mixing is mainly due to the combined effect of unbalanced collisions of the fluid streams and Dean vortices. The micromixer shows interesting mixing behavior for different ratios of the widths of the two split sub-channels. The sub-channels wherein the major sub-channel is twice as wide as the minor sub-channel exhibit the highest mixing performance at Reynolds numbers larger than 40. The results show the lowest mixing performance for the case of uniform width, where balanced collisions occur.

1. Introduction

Microfluidics is an interdisciplinary branch of physics and engineering that deals with the study of fluid flows in sub-millimeter channels [1]. A microfluidic system for biological or chemical analysis is also known as a 'lab-on-chip' or 'micrototal analysis system (μTAS)' because this system can perform various biochemical processes in a micro-scale chip. It has wide applications in chemical analysis [2, 3], clinical and forensic analysis [4, 5] and DNA sequencing [6–8]. The typical functions performed on a microfluidic device involve processes such as sample preparation and homogenization, separation and detection. These devices comprise many microscale components such as microchannels, micropumps, micromixers and microvalves. Micromixers are an important component of microfluidic systems that are needed for the homogenization of the sample reagents.

The liquid flow in most microfluidic devices is restricted to the laminar-flow regime due to low Reynolds numbers [9], which are far below the threshold for turbulence. Mixing at a macro-scale is facilitated by the presence of turbulence in the flow. The absence of turbulence in these microfluidic devices makes it difficult to mix the fluids. The mixing of the different fluid streams in a simple smooth microchannel is mainly governed by the diffusion of molecules, and diffusive mixing is very slow and inefficient compared to convective mixing. The rapid mixing of fluids in such microdevices is critical in a variety of applications. Recently, numerous micromixing devices have been developed to overcome the problem of mixing. Micromixers can be generally classified as active or passive micromixers. Detailed reviews of the design and operating principles of various active and passive micromixers are reported in the literature [10–12].

An active micromixer uses moving parts or an external source of energy to enhance the mixing of fluid samples. The external sources of energy are pressure field disturbances, electric fields and magnetic fields. Although active micromixers are very effective in mixing, they are difficult to fabricate and integrate with microfluidic systems.

[1] Author to whom any correspondence should be addressed.

Furthermore, the operation of active micromixers with moving parts is also difficult due to the interaction of impurities with systems of small dimensions.

Passive micromixers do not require any external energy sources and mix the fluids by a special geometry that creates a specific flow field. Unlike active micromixers, the designs of passive micromixers are often simpler; hence, they are easy to fabricate and integrate with microfluidic systems. Some of the recently developed passive mixers with channel designs that show efficient mixing performance are zig-zag [13, 14], serpentine [15] and curved channels [16]. Johnson *et al* [17] and Stroock *et al* [18] reported a novel design by creating grooves on the wall of the channel that yield efficient mixing. Wang *et al* [19] proposed the intersection of two patterned channels that cross over each other, akin to a rhombus. However, the design was not aimed to harness the effect of the collisions of fluid streams for enhancing the mixing performance.

There are some basic designs of the micromixer based on the concept of the collision of fluid streams. The simplest passive micromixer in which two separate fluid streams are brought into contact from opposite directions and then leave though a channel that is perpendicular to the inlet channels is the T-mixer [20]. However, after a certain distance from the T-joint of the mixer, the flow in a simple, straight channel becomes a simple, laminar flow, and hence, does not significantly contribute to mixing.

Chung and Shih studied both experimentally and numerically a planar micromixer with rhombic microchannels [21, 22]. The microchannels were designed on the concept of 'split and recombine' to create a collision of fluid streams. The study was undertaken with regard to sub-channels of equal width, which generate balanced collisions. Mouza *et al* [23] investigated the mixing performance of a micromixer that splits and recombines with curved microchannels. The micromixer was designed to keep the main channel as well as the sub-channels in curved shape to induce Dean vortices. The width of the split sub-channels was uniform, and hence caused a balanced collision of the fluid streams. The curve design of the micromixer explored the possibility of enhancing mixing performance by Dean vortices. The strength of the Dean vortices for a given Reynolds number (Re) is described by a non-dimensional parameter called the Dean number defined as $K = Re(D/R)^{1/2}$, where D and R are the characteristic dimension and the radius of curvature of the channel, respectively. The formation of Dean vortices induces secondary flows in the form of two counter-rotating vortices which modulate the interface of the fluid streams to increase mixing.

The direct collision [20, 23] and the cross-collision [21, 22] of fluid streams in a microchannel with a uniform width do not alter the interface between the fluids over which mixing takes place. These collisions result in the formation of a clear and thin interface between the fluids. The micromixers with rhombic microchannels utilize the constriction in the flow to increase mixing. In these rhombic designs, higher mixing is mainly due to constriction. But the idea is not new for the rhombic micromixers because providing constriction to the flow in any microchannel will increase mixing performance as it reduces the length of diffusion for fluid molecules to be mixed. If the constriction in a rhombic micromixer is assumed to be removed, the interface is likely to be present only near the zone where the sub-channels recombine after which the two fluids separate into the sub-channels on their respective sides, where no mixing takes place. In the design of such micromixers, only a single fluid flows in the sub-channels due to the balanced collision of the fluid streams and splitting and collision are not likely to play any special role in enhancing the mixing of the fluids. Some effort should be aimed at exploiting the collision of the fluid streams for enhancing the mixing of the fluids. The collision of the fluid streams should be effective in repeatedly altering the interface between the fluids during their flow in the micromixer. With this motivation, the unbalanced, cross-collision of fluid streams has been investigated at low Reynolds numbers.

In the present study, a novel design of the micromixer that is based on the concept of unbalanced splits and cross-collisions of fluid streams is proposed and fabricated. The micromixer has been analyzed both experimentally and numerically for a range of Reynolds numbers (10–80) lying in the laminar flow regime. The main channel is split into two sub-channels of unequal widths and then recombined after a certain distance in a repetitive fashion. The difference in the inertia of the fluid flow in the split channels by the unequal widths creates an unbalanced collision, which perturbs the flow and shifts the interface of the fluid streams into the sub-channel where Dean vortices become effective in enhancing mixing, which is very effective for mixing as compared to a balanced collision. The effects of the ratio of the widths on mixing and flow behavior have been investigated at various Reynolds numbers.

2. Physical model of the micromixer

Figure 1(a) shows a schematic model of the proposed micromixer based on the concept of unbalanced splits and cross-collisions of fluid streams. The two fluids separately enter through two different inlets and come into contact at a T-joint where they undergo some mixing before entering the micromixer and thence to a series of sub-channels. The channel is split into two sub-channels of unequal widths and then recombined after a certain distance in a repetitive manner. The rate of mass flow in the major sub-channel, i.e. the sub-channel with larger width, is greater than that in the minor sub-channel. Hence, the inertia of the fluid in the major sub-channel is higher than that of the fluid in the minor sub-channel. The thick arrow line indicates the path of the major flow stream. The difference between the inertias in the major and minor sub-channels creates an unbalanced collision of fluid streams. After each collision, the major sub-channel changes its position across the x-axis.

An optical micrograph of the micromixer is shown in figure 1(b). Experimental and numerical analyses have been carried out on the models of the micromixer that comprise six segments of splitting and recombination, respectively. The number of the mixing segments was kept as 4 for simulations

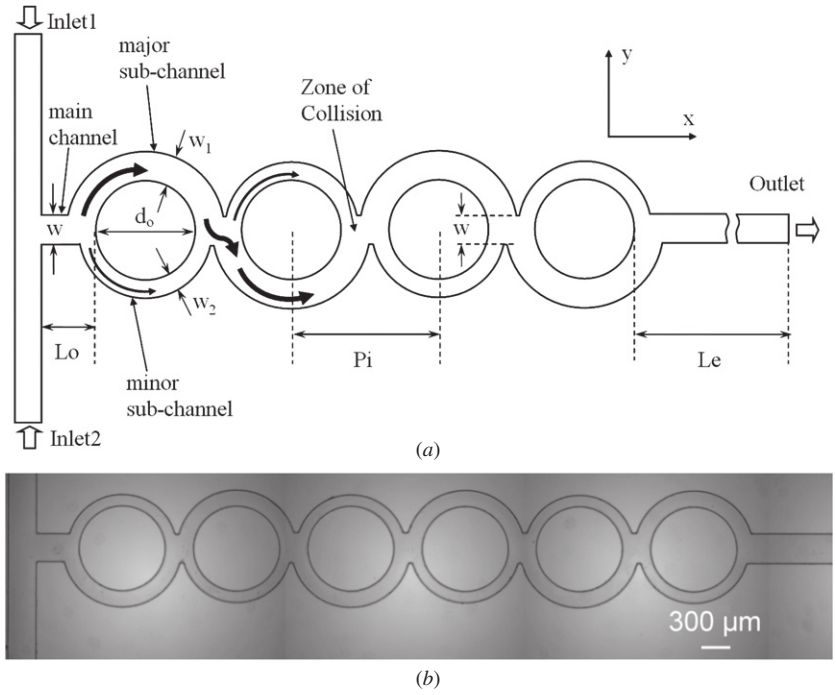

Figure 1. Micromixer based on unbalanced splits and cross-collisions: (*a*) schematic diagram and geometric parameters and (*b*) optical micrograph of the micromixer captured from the top view for $w_1/w_2 = 1.4$.

considering computational time and storage. The pitch, *Pi*, is fixed as 1.2 mm. The widths of the two sub-channels are w_1 and w_2, respectively. The sum of the widths of the two sub-channels is equal to the width of the main channel, w, which is fixed as 300 μm, i.e. $w_1 + w_2 = w = 300$ μm. The widths of the sub-channel are controlled by changing the position of the outer wall relative to a fixed inner wall. The height of the micromixer, h, for the experiments and the numerical calculations has been fixed at 120 μm. The diameter of the inner wall, d_o, is fixed at 900 μm for circular sub-channels. The different axial lengths of the channel shown in figure 1(*a*) are given as $Lo = 500$ μm and $Le = 2.95$ mm.

3. Numerical analysis

The flow and the mixing in the proposed micromixer that utilizes the concept of unbalanced splits and cross-collisions of fluid streams have been numerically analyzed by numerically solving three-dimensional continuity and Navier–Stokes equations. The governing differential equations are discretized by the finite-volume method via a coupled solver [24]. The flow is assumed as being at the steady state and incompressible. No-slip boundary conditions are applied on the solid walls.

In the case of multi-component fluids, the fluids are assumed to mix at the molecular level and to have the same mean velocity and pressure. It is also assumed that the mass transfer takes place by convection and diffusion. Hence, the bulk motion of the fluid is modeled by using a single velocity and pressure, while each component has its own equation for the conservation of mass. For each control volume in the flow domain, the appropriate average values of the properties are evaluated for calculating the flow field. These average values depend on the properties of the fluid components and the proportions of the fluids in the control volume. The differential motions of the individual components in the mixture are accounted for by the relative mass flux term. This term may be modeled in a number of ways to include the effects of concentration gradients and pressure gradients. The concentration gradient is the primary effect of the possible relative motion of the mixture components.

Hexahedral grids have been constructed for the full model. A high-quality mesh is critical to achieve accurate numerical results, especially for mixing analyses. In comparison with unstructured meshing for analysis, structured meshing offers the advantage of better control in completely packing all the corners with a sufficient number of nodes. In the present study, a structured mesh is used for all geometries.

With reference to the boundary conditions, normal velocities are specified at the two inlets, and zero static pressure is set at the outlet. The Reynolds number is evaluated by considering the width of the main channel, w, as the characteristic length and water as the working fluid. The mixing analysis has been carried out with two fluids, i.e. ethanol and water, which enter the micromixer from Inlet1 and Inlet2, respectively. The main reason for selecting water and ethanol is that there are a number of studies on mixing with these fluids. The second reason is that these two practical fluids which can be selected for carrying out numerical simulation for evaluating mixing with the physical properties, especially diffusivity, are quite suitable for numerical analysis. The volumetric flow rates at these two inlets are the same. The geometric parameter, w_1/w_2, is varied from 1.0 to 3.0. In all, six Reynolds numbers are considered from 10 to 80. The

properties of water and ethanol are measured at 20 °C. The diffusivity of water and ethanol is 1.2×10^{-9} m^2 s^{-1}, and the densities of water and ethanol are 9.97×10^2 and 7.89×10^2 kg m^{-3}, respectively. The viscosity of water and ethanol are 0.9×10^{-3} and 1.2×10^{-3} kg m^{-1} s^{-1}, respectively. The numerical solutions are considered to have attained convergence when the root-mean-square (RMS) residual value is 10^{-6}.

4. Quantification of mixing

To quantify and analyze mixing, the variance of the fluid species in the micromixer has been calculated. The variance of the species is determined in a cross-sectional area of the micromixer that is perpendicular to the x-axis. The variance is based on the concept of the intensity of segregation, which is based on the variance of the concentration in relation to the mean concentration. To evaluate the degree of mixing in the micromixer, the variance of the mass fraction of the mixture in a cross-section that is normal to the direction of flow is defined as

$$\sigma = \sqrt{\frac{1}{N}\sum_{i=1}^{N}(c_i - \bar{c}_m)^2}. \quad (1)$$

In equation (1), N is the number of sampling points inside the cross-section, c_i is the mass fraction at the sampling point i and $\bar{c}_m$ is the optimal mixing mass fraction. The number of sampling points, N, on each plane was kept more than 400 to ensure high accuracy in the value of the mixing index. The sampling points are equidistant on the cross-sectional plane. The values at the sampling points are obtained by interpolation with the values at adjacent computational grids. For evaluating the degree of mixing of the fluids on a plane that is perpendicular to the direction of flow, the mixing index at an axial location is defined as follows:

$$M = 1 - \sqrt{\frac{\sigma^2}{\sigma^2_{\max}}}. \quad (2)$$

In equation (2), $\sigma_{\max}$ is the maximum variance over the range of data. The variance is maximal for completely unmixed fluids and minimal for completely mixed fluids. M_o denotes the value of the mixing index at 5.5 mm downstream of the end of the last sub-channels.

5. Device fabrication and experiment

The polydimethylsiloxane (PDMS) replica molding method was used to fabricate the micromixer. It involves preparing the SU-8 resist mold over a silicon wafer by photolithography and transferring the pattern of the micromixer to PDMS replica. Initially a 6″ silicon wafer was air-cleaned and dehydrated at 96 °C for 2 min. A 120 μm thick layer of negative photo resist (SU-8 2075 MicroChem, MA, USA) was spin coated on the silicon wafer by a spin coater at 2100 rpm for 30 s and soft baked. UV light was exposed to the coated wafer through a high resolution dark film mask with a filter by a standard UV aligner with wavelength (365 nm) and exposure energy 248 mJ cm^{-2} (35 s at 6.8 mW cm^{-2}) and proceeded to post-bake. After using the SU-8 developer the SU-8 resist mold was developed to take off unexposed SU-8. The PDMS solution (the mixture of the Sylgard 184 silicon elastomer and the curing agent with a 10:1 ratio by weight) was poured onto the patterned Si-wafer, degassed by the vacuum desiccator (H42050, Bel-Art product, NJ, USA), and then cured at 70 °C for 2 h. Holes for the inlet and the outlet were punched in the PDMS replica after peeling off from the SU-8 resist mold. A Teflon tube was used to connect the inlet and outlet holes of the micromixer by compressive fitting harnessing the flexibility of the PDMS mold and the Teflon tube. The diameters of the holes and the connecting tubes were commonly 1.5 mm. The dimension of the channel of the micromixer in the final PDMS channel was checked at several positions by the surface profilometer, and the average depth of the channels was equal to 120 μm. The PDMS replica channel was sealed to a standard microscope slide (1″ × 3″) using oxygen plasma treatment (CUTE-100LF, FEMTO Science, Hwasung, Korea). The slide was properly cleaned with acetone before oxidizing the surface of the PDMS replica and the glass slide for 1 min to make irreversible sealing. Some micromixers have complicated design and microstructure in the channel which needs complicated multistage fabrication and precise alignment. The present design of the micromixer has simple geometry and is fabricated in the one-step photolithography technique.

The fluorescence measurement technique is used for evaluating mixing performance in the microchannel [25]. Mixing experiments have been carried out with ethanol and distilled water (Milli Q purified) labeled with Rhodamine B (fluorescent solution) 100 μM concentration taken as the working fluid. The diffusion coefficient of Rhodamine B in water [17, 26] and ethanol [27, 28] is 2.8×10^{-10} m^2 S^{-1}. Before each experiment the fluorescent solution was well mixed by the vortex mixer (KMC-1300V, Vision Scientific Co., Ltd, Kyeonggi-do, Korea), and then both fluids were filtered using the syringe filter. The two fluids were introduced into the micromixer using two syringes connecting to the inlet of the micromixer by the Teflon tube. A multifeed syringe pump (Model 200, Kd Scientific Inc., MA, USA) was used to establish a controlled and continuous flow in the micromixer by pumping the fluids using two separate syringes. The volumetric flow rate was maintained corresponding to the different Reynolds numbers. The range of Reynolds numbers considered for experimental analysis was from 10 to 80.

Mixing of the fluids was analyzed by capturing the top view images and image processing with the NIH ImageJ software. Images were obtained using an inverted fluorescence microscope (Ti-u, Nikon, Tokyo, Japan) integrated with a Nikon CCD camera. Both qualitative and quantitative analyses have been carried out to understand the mechanism of mixing in the micromixer. Background noise corrections were performed to correct for the distribution of illumination intensity from the UV lamp. Top view images of mixing represent the average concentration distribution over a certain depth of the channel. The fluorescence intensity in the image has been evaluated on a line positioned perpendicular to the

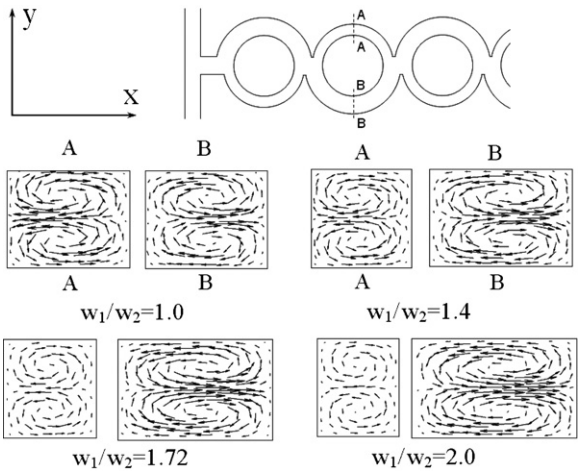

Figure 2. Predicted velocity vectors on the *yz*-plane with different ratios of w_1/w_2 at $Re = 60$.

direction of flow with the length equal to the width of the main channel. The value of the intensity of the image was normalized by the highest and lowest values using the equation

$$I_{ni} = \frac{I_i - I_{\min}}{I_{\max} - I_{\min}}, \tag{3}$$

where I_i is the local intensity on the line, and $I_{\min}$ and $I_{\max}$ are the minimum and maximum values of the intensity, respectively. This normalized value of intensity was used to calculate the standard deviation from the mean value. Finally, the mixing index was evaluated from the value of the standard deviation using equation (2).

6. Results and discussion

A new passive micromixer based on the concept of unbalanced splits and cross-collisions of fluid streams has been proposed and fabricated using the soft lithography technique. Experimental and numerical analyses have been performed to investigate the mixing performance of the micromixer for Reynolds numbers ranging from 10 to 80. In order to perform numerical simulations, the preliminary grid independence test has been carried out with five different grid systems, for circular sub-channels with $w_1/w_2 = 2.0$. The distribution of the mixing index has been evaluated on planes across the direction of flow along the *x*-axis for various grid systems. The grid system with 2.5×10^6 nodes has been selected as the optimum grid system on which further analyses are performed. The optimum grid system has 35×30 nodes on a typical cross-sectional plane (*yz*-plane) in the sub-channel and 135 nodes along each sub-channel length. The number of nodes on a cross-section in the main channel (split and recombine zone) of the micromixer is 55×30. The mesh density is adjusted so that it becomes higher near the regions where the splitting and cross-collision take place.

6.1. Flow analysis

The flow structure in the micromixer contributing to mixing is described in this section. Figure 2 shows the numerical results for the velocity vectors on the *yz*-plane at a fixed axial position with different ratios of w_1/w_2 at $Re = 60$. The secondary flows between the major and minor sub-channels differ in terms of strength. The difference continuously decreases as the level of imbalance of the widths decreases. The sub-channels with equal width show almost equal and similar secondary-flow structures in both sub-channels. Although a strong transverse flow is present in both sub-channels, low mixing is depicted in this geometric configuration. In this case, mixing is due only to the Dean vortices that are present in the sub-channels. However, in the case of unbalanced cross-collisions, due to the difference in the inertial forces of the two fluids in the sub-channels, the collisions are effective in perturbing the interface between the fluids.

Figure 3 shows the numerical results for the development of the mass-fraction distribution of ethanol on the *yz*-plane along the axial length of the micromixer for $w_1/w_2 = 1.0$, 1.4, 1.72 and 2.0, at $Re = 60$. In the case of balanced collision (sub-channels with equal widths, i.e. $w_1 = w_2$), a sub-channel is almost occupied by a single fluid, and the proportion of the single fluid is the same in both the sub-channels. In this case, there is no significant change in the mass-fraction distribution along the axial length of the micromixer. This means that the balanced collisions rarely affect the mixing. However, in the cases of unbalanced collision ($w_1/w_2 = 1.4$, 1.72 and 2.0), the area of the interface in main channels is seriously distorted due to vortical transverse flows. Although the shape of the mass-fraction distribution significantly differs between the second and third sub-channels (planes 1 and 2) in the case of unbalanced collision, the shapes of the distributions in the third and fourth sub-channels (planes 2 and 3) are nearly the same, regardless of the ratio of widths. This means that the mass-fraction distribution is fully established at the third sub-channel. The perturbation in the area of the interface between the fluids is due to the presence of the Dean vortices in the sub-channels. The area of the interface in the main channel increases as the ratio of widths increases. Overall qualitative comparison of the mass-fraction distributions for various ratios of w_1/w_2 shows that the mixing performance is improved as the ratio of widths increases, as depicted in figure 8. The degree of mixing increases with the level of imbalance of the collisions.

Figure 4 shows the numerical results for the projected streamlines of two different fluids that enter from Inlet1 and Inlet2, respectively, and pass through the sub-channels of the micromixer. In the case of balanced collision ($w_1 = w_2$) that is shown in figure 4(*a*), the streamlines seem nearly symmetric. The streamlines that are initiated from two different inlets come into contact only in the splitting–collision zones. The streamlines continue to follow the path along their own side after collisions. Thus, the chance of mixing is quite limited in comparison with the above unbalanced case. Figure 4(*b*) represents the case of unbalanced splitting and collision for $w_1/w_2 = 2.0$ at $Re = 60$. Since the major sub-channel has a larger cross-sectional area, the water from Inlet2 is divided into two streams: one enters the first major sub-channel and the other enters the minor sub-channel on the side of Inlet2. However, the ethanol stream entirely flows into the major sub-channel on its side. Since the strength of secondary flows in

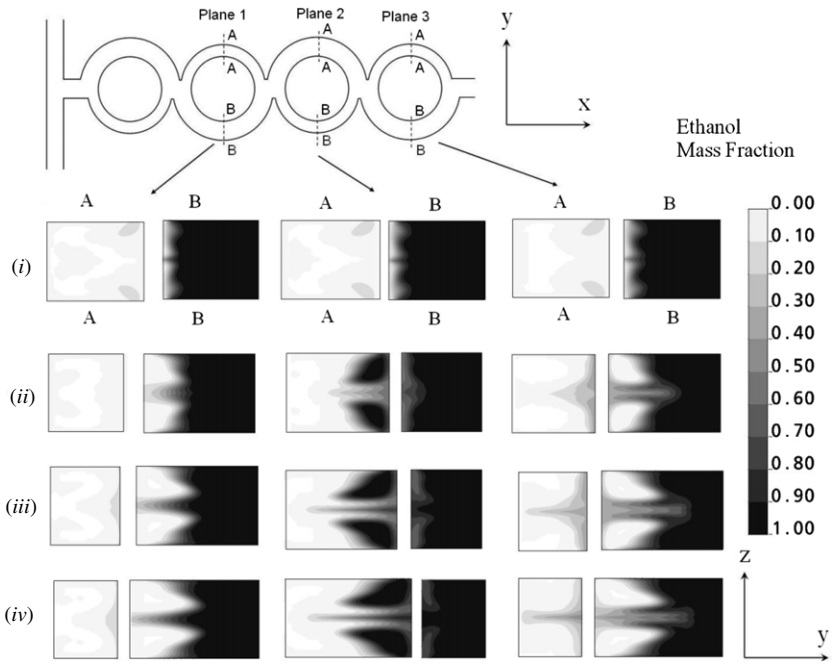

Figure 3. Predicted mass-fraction distributions at $Re = 60$: (*i*) $w_1/w_2 = 1.0$; (*ii*) $w_1/w_2 = 1.4$; (*iii*) $w_1/w_2 = 1.72$ and (*iv*) $w_1/w_2 = 2.0$.

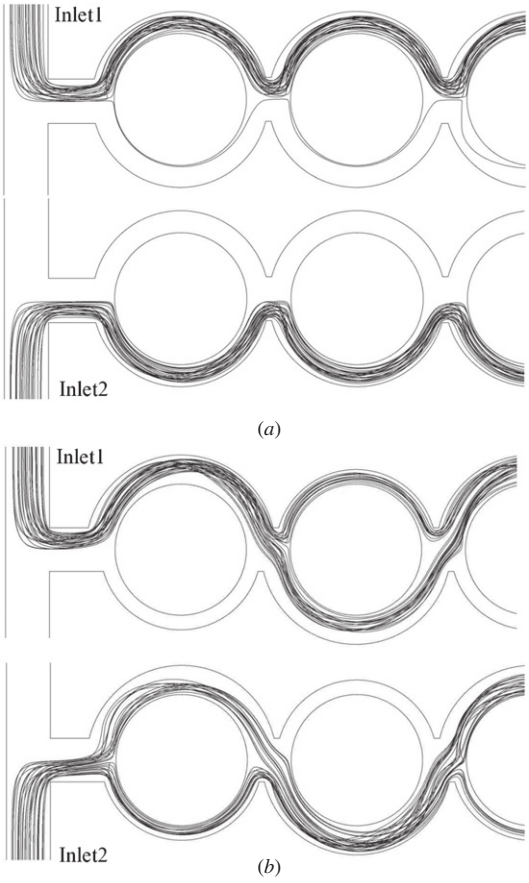

Figure 4. Predicted projected streamlines from Inlet1 and Inlet2 at $Re = 60$: (*a*) balanced collisions, $w_1/w_2 = 1.0$ and (*b*) unbalanced collisions, $w_1/w_2 = 2.0$.

the major sub-channel and the inertia of ethanol is larger than that of water in the first major sub-channel (due to the larger

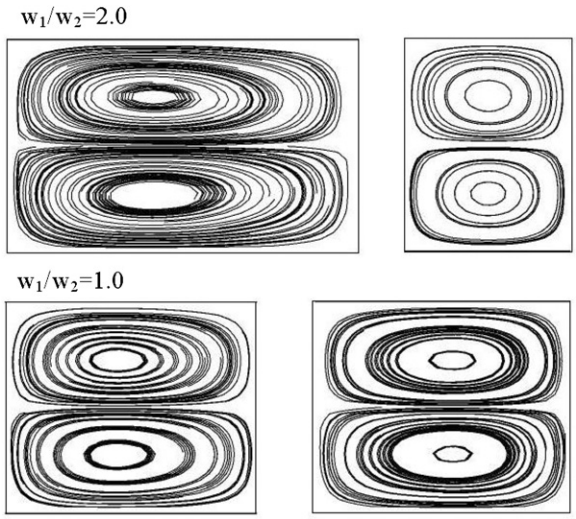

Figure 5. Streamlines on the cross-sectional plane at the center of the first mixing segment to show the Dean vortices as a function of the w_1/w_2 ratio at $Re = 60$.

rate of flow of ethanol in this sub-channel), the ethanol stream pushes the two water streams through collision at the inlet of the second sub-channels. As a result, the two water streams enter into the second major sub-channel as a single stream, as shown in figure 4(*b*). The ethanol stream is divided into two streams and goes into the second major sub-channel and into the minor sub-channel on its side. This pattern is repeated downstream.

Figure 5 shows the streamlines on a cross-sectional plane (*yz*-plane) at the center of the first mixing segment in both sub-channels for balanced ($w_1/w_2 = 1.0$) and unbalanced collisions ($w_1/w_2 = 2.0$) at $Re = 60$. A pair of vortices can be visualized in both circular sub-channels. For balanced

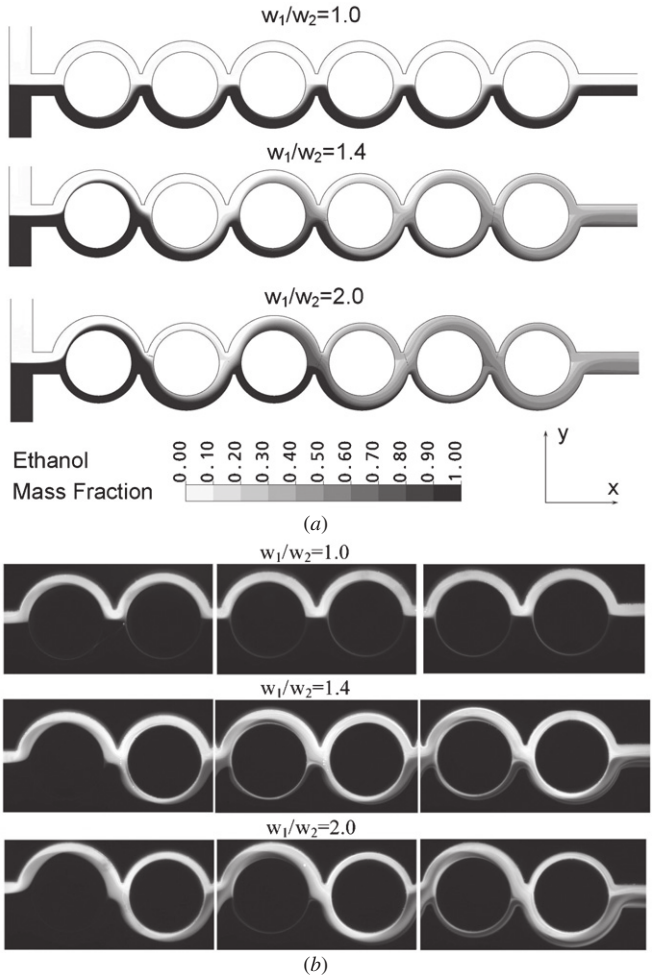

Figure 6. Results for distribution of the mass-fraction of ethanol as a function of w_1/w_2 at $Re = 60$: (*a*) numerical simulation results on the *xy*-plane that is midway along the channel height and (*b*) experimental results, top view optical images captured by the CCD camera showing mixing of fluids.

collisions, the Dean number for the flow in sub-channels is 30 while for unbalanced collision the Dean number in major and minor sub-channels ($w_1/w_2 = 2.0$) is 31 and 26, respectively. The streamlines in the sub-channels can be compared with the streamlines reported for a helical microchannel by Schönfeld and Hardt [29]. The structure of the Dean vortices of the present simulation is similar to their results at the Dean number 150.

6.2. Mixing analysis

Qualitative comparison between numerical and experimental results for mixing is shown in figures 6(*a*) and (*b*) for different values of the w_1/w_2 ratio. Numerical simulation results show the mass-fraction distributions of ethanol on the *xy*-plane in the cross-section that is midway along the channel height of the micromixer. The effect of the ratio of widths on mixing is shown for three values of w_1/w_2, namely, 1.0, 1.4 and 2.0, at $Re = 60$, in which $w_1/w_2 = 1.0$ corresponds to the case of balanced collision of the fluid streams. The flows from the two sub-channels undergo splitting and collision. In the case of equal widths, the interface of the two fluids almost coincides with the plane of symmetry of the micromixer. Thus, the area of the interface is restricted to only the splitting–collision zones. This phenomenon is also shown in experimental results. On the other hand, the contour-plots for $w_1/w_2 = 1.4$ and 2.0 correspond to unbalanced collisions of fluid streams. In this case, the interface of the two fluids is not restricted to the small regions of splitting and collision, but extends to the full length of the sub-channels of the micromixer. This is attributed to unbalanced cross-collisions. Unlike the case of balanced collision, the interface of the two fluids is clearly seen in the sub-channels; the increased area of the interface enhances the mixing.

Experimental results for the effect of balanced and unbalanced collisions of fluid streams on mixing are shown in figure 6(*b*). Each snapshot covers only two mixing segments of the micromixer due to the limited viewing area of the microscope. Hence a total of three snapshots were taken and aligned to show the full length of the micromixer. The interface of the fluid streams before the inlet to the first mixing segment is very clear and thin for all cases. For balanced collision of fluid streams ($w_1/w_2 = 1.0$), the interface of the fluid streams at the exit of the last mixing segment of the micromixer is still very clear and thin without any deformation. In this case, poor mixing is depicted as the streams of similar fluids symmetrically split in equal volumes in the sub-channel in a repetitive fashion in all six mixing segments of the micromixer. In the case of unbalanced collision, the micromixer shows efficient mixing performance as can be visualized at the exit of the last mixing segment. The result of numerical simulation qualitatively agrees well with the experimental result in the case of balanced collision ($w_1/w_2 = 1.0$), and reasonably in the cases of unbalanced collision ($w_1/w_2 = 1.4$ and 2.0).

The mechanism of mixing in the micromixer can be understood from the results of the flow field presented in figures 2, 3 and 6. Although Dean vortices are present in both sub-channels for balanced as well as unbalanced collisions of the fluid streams, poor mixing is depicted by the balanced collision due to the presence of only single fluid in sub-channels. In the case of unbalanced collisions of the fluid streams, the collisions perturb the flow and shift the interface of the fluid streams into the sub-channels where the Dean vortices become effective in mixing. The mixing in the present micromixer is due to the combined effect of unbalanced collisions of the fluid streams and Dean vortices.

The differences between the experimental and computational results are likely to arise due to the difference in the value of the diffusion coefficient of the fluids and the fluorescent, difference in the observation of the concentration profiles and also due to the geometrical variations. In the present experiment, two different fluids, water and ethanol, are considered for evaluating the mixing performance of the micromixer using Rhodamine B as a fluorescent mixed with water. The special distribution of water (with Rhodamine B) and ethanol is used to visualize and evaluate mixing performance of the micromixer. The diffusion coefficient of Rhodamine B in water and ethanol and that

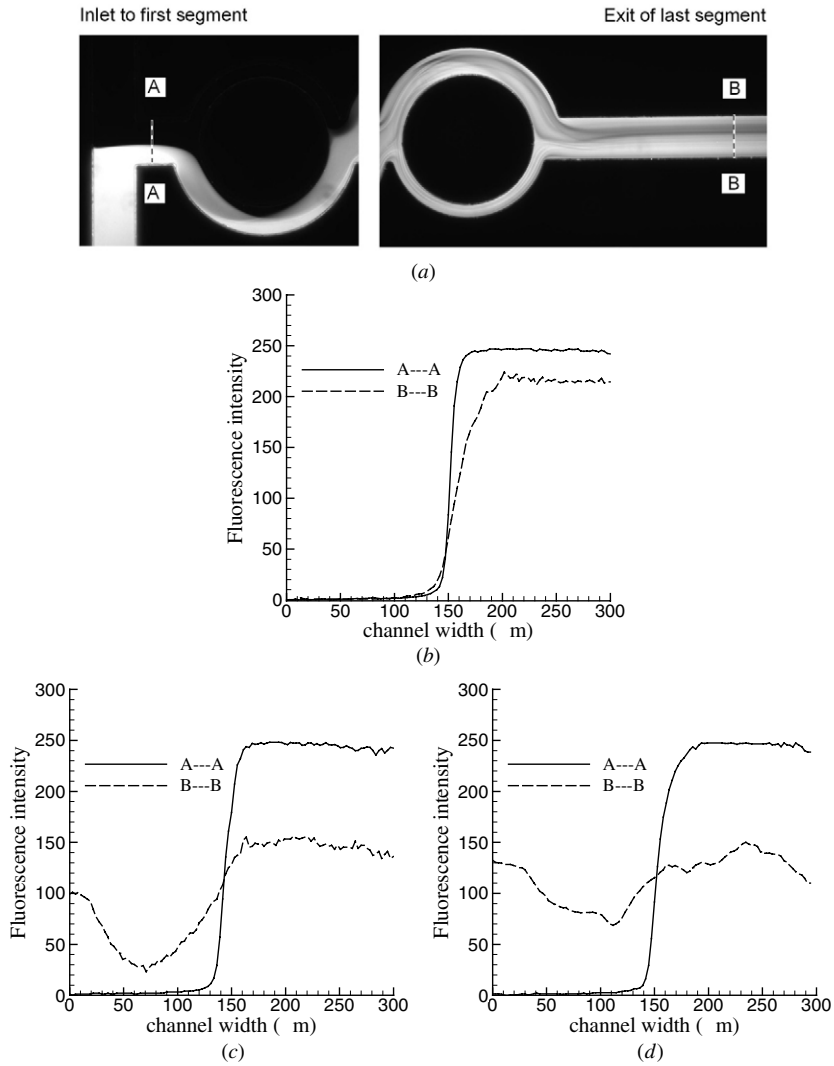

Figure 7. Experimental results: (*a*) representative images showing mixing of fluids in the first and last mixing segments respectively for $w_1/w_2 = 2.0$ and $Re = 80$; plots for the fluorescence intensity across the width of the channel at two positions (A–A) and (B–B), (*b*) balanced collisions of fluid streams ($w_1/w_2 = 1.0$, $Re = 60$) and unbalanced collisions ($w_1/w_2 = 2.0$), (*c*) $Re = 60$ and (*d*) $Re = 80$.

of water in ethanol will affect the experimental results. The diffusivity of Rhodamine B in water [17, 26] and ethanol [27, 28] is 2.8×10^{-10} m^2 s^{-1} which is lower than the diffusivity of the water in ethanol (1.2×10^{-10} m^2 s^{-1}). The Rhodamine B and water will mix with ethanol at different rates due to the difference in the diffusion coefficient. The diffusion coefficient of Rhodamine B is equal for water and ethanol, and hence will diffuse at the same rate in both fluids. The diffusion coefficient of Rhodamine B in ethanol is less than the diffusion coefficient of water in ethanol. The results will show lower mixing as compared to the actual mixing of water and ethanol. The second reason for the differences between the experimental and computational results can be two-dimensional observation of the concentration profile which gives an average value over a certain depth of focus, and mixing is evaluated by concentration distribution on a line across the flow (figure 7(*a*)). In numerical simulation, mixing is evaluated using the two-dimensional concentration profile on the plane at a specific position. The difference in the geometry of the micromixer used for experiment and simulation could also be one of the reasons for the difference in the mixing results. The model used in simulation is accurate to the assigned dimensions; the wall is free from any artifacts and operates under an ideal condition. However, in the case of the experiment model, the wall surface is not completely smooth, and also the geometry is not exact to the dimension as the height of the micromixer was 120 ± 2 μm as measured by the profilometer. In addition, the SU-8 resist mold is not likely to be perfectly developed to the desired uniform dimensions. Thus, the rough wall and the variation of dimension in the experimental model are also important sources for the difference between the results.

The analyses of the experimental results are represented in figure 7 by comparing the fluorescence intensity between two different positions in the micromixer. Figure 7(*a*) shows the magnified images of the first and sixth mixing segments for unbalanced collision of fluid streams ($w_1/w_2 = 2.0$). Variations of the fluorescence intensity have been evaluated by analyzing the images at two fixed positions, A–A and B–B, respectively. The plots of the fluorescence intensity for

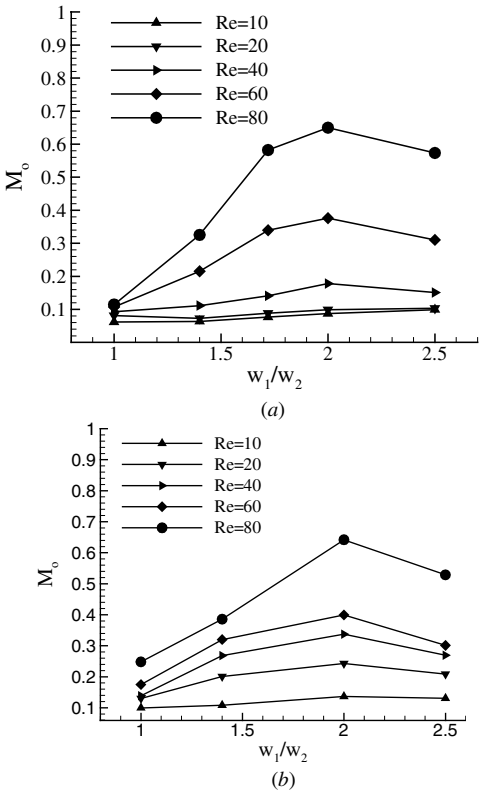

Figure 8. Evaluation of mixing performance: the mixing index at the end of the micromixer M_o versus w_1/w_2 at various Reynolds numbers. (*a*) Numerical simulation: M_o is evaluated using the mass fraction distribution on a plane perpendicular to the direction of flow. (*b*) Experimental results: M_o is the mixing index evaluated at position B–B shown in figure 7(*a*) using the value of the fluorescence intensity in grayscale image along line B–B.

balanced ($w_1/w_2 = 1.0$) and unbalanced collisions ($w_1/w_2 = 2.0$) of fluid streams are shown in figures 7(*b*), (*c*) and (*d*), respectively. At the inlet of the first mixing segment (position A–A), the fluorescence intensity sharply changes (in step) from the lowest value to the highest value across the interface of the fluid streams. In the case of balanced collision, there is only little change in the profile of the intensity at the exit of the channel (position B–B) in comparison with that at A–A. This result indicates low mixing performance of the balanced collision of the fluid streams. However, the change in the profile of fluorescence intensity at the exit (position B–B) for the case of unbalanced collision is remarkable as shown in figures 7(*c*) and (*d*) for $Re = 60$ and 80 respectively. As Reynolds number increases from 60 to 80, the intensity becomes more uniform, which represents good mixing achievement.

The mixing performance of the micromixer has been evaluated for different Reynolds numbers by both numerical simulation and experiment as shown in figures 8(*a*) and (*b*), respectively. Figure 8(*a*) shows the results of numerical simulation for the mixing performance as a function of w_1/w_2 for Reynolds numbers ranging from 10 to 80. The unbalanced collision is effective in mixing the fluids for all the Reynolds numbers that are investigated in the present study. The mixing index shows the maximum value at $w_1/w_2 = 2.0$, for all the

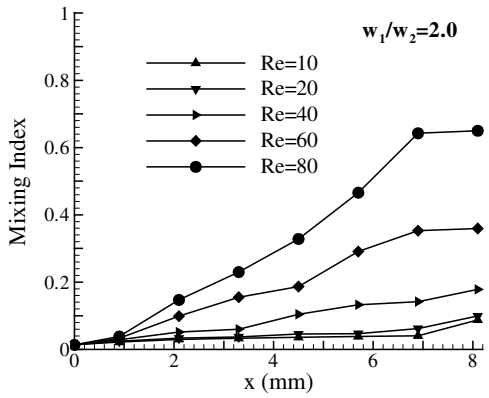

Figure 9. Mixing characteristics along the axial length for the representative geometry $w_1/w_2 = 2.0$ as a function of the Reynolds number.

Reynolds numbers except 10. It is obvious that the unbalanced collision is not so effective for low Reynolds numbers due to the low inertial forces at such numbers and hence the present micromixer might not be suitable for those microfluidic devices operating in such a regime of the Reynolds number. However, even at very low Reynolds numbers, the unbalanced collision of fluid streams shows better mixing performance as compared to balanced collision ($w_1 = w_2$).

The experimental results have been analyzed to evaluate the mixing index at the exit of the last mixing segment; position B–B (shown in figure 7(*a*)). The variations of the mixing index with w_1/w_2 are shown for five Reynolds numbers in the figure. These variations agree qualitatively well with those obtained by numerical simulation shown in figure 8(*a*), but show some discrepancies quantitatively. These discrepancies are due to the differences in geometry between experiment and numerical simulation, and also to the numerical and experimental errors.

The mixing characteristics of the micromixer along the channel is shown in figure 9 for $w_1/w_2 = 2.0$ at different Reynolds numbers. The mixing index has been evaluated on cross-sectional planes located at the inlet and the exit of the circular mixing segment and at the central positions of all six circular mixing segments. The micromixer shows nearly identical and relatively low rate of mixing along the channel length for $Re = 10$ and 20. The rate of mixing, however, increases rapidly beyond the Reynolds number, 40, which shows that the micromixer is effective in rapid mixing at higher Reynolds numbers. The result gives an idea about the length of the micromixer required to attain complete mixing of the fluid.

7. Conclusions

A novel design of passive micromixers based on the concept of unbalanced splits and cross-collisions of fluid streams has been proposed. The main channel is split into two sub-channels of unequal widths that subsequently recombine after a certain distance. The difference in the rate of mass flow in the two sub-channels creates an unbalanced collision of the two fluid streams which perturbs and shifts the interface of the fluid streams into the sub-channel. The interface in the curved sub-channels harnesses Dean vortices in enhancing mixing

performance of the micromixer. Experimental and numerical studies have been conducted to investigate mixing and the flow field Reynolds numbers ranging from 10 to 80. The numerical results for the mixing index qualitatively show quite good agreement with the experimental results. More depth studies by numerical simulation also show the mixing mechanism of the micromixer enhancing performance by the development of Dean vortices in the sub-channels. The split channels, wherein the width of the major sub-channels is twice that of the minor sub-channels (i.e. $w_1/w_2 = 2.0$), show the highest mixing performance at Reynolds numbers larger than 20. The result shows the lowest mixing performance for sub-channels of equal width (balanced collision) at all Reynolds numbers. The mixing index increases with the ratio of the width of the major sub-channel to the minor sub-channel.

This novel design of the micromixer can be a possible component of a lab on chip or a microfluidic system because this mixer can be fabricated by a simple process and effectively increases the mixing of two fluid streams. The design concept of the present micromixer can be extended to other possible designs of split and recombine micromixers. Further work will be focused on understanding the mechanism of distortion of the interface of the fluid streams by unbalanced collisions of the fluid streams and its relation to mixing.

Acknowledgments

This research was supported by the National Research Foundation of Korea (NRF) grant no 2009-0083510 funded by the Korean government (MEST) through Multi-Phenomena CFD Engineering Research Center. This work was also supported by National Research Foundation of Korea Grant funded by the Korean Government (2009-0065065) for Khalid Anwar.

References

[1] Stone H A, Stroock A D and Ajdari A 2004 Engineering flows in small devices: microfluidics toward a lab-on-a-chip *Ann. Rev. Fluid Mech.* **36** 381–411
[2] Manz A, Graber N and Widmer H M 1990 Miniaturized total chemical analysis systems: a novel concept for chemical sensing *Sensors Actuators* B **1** 244–8
[3] Jensen K F 1999 Microchemical systems: status, challenges, and opportunities *AIChE J.* **45** 2051–4
[4] Verpoorte E 2002 Microfluidic chips for clinical and forensic analysis *Electrophoresis* **23** 677–712
[5] Pal R *et al* 2005 An integrated microfluidic device for influenza and other genetic analyses *Lab Chip* **5** 1024–32
[6] Effenhauser C S, Bruin G J M, Paulus A and Ehrat M 1997 Integrated capillary electrophoresis on flexible silicone microdevices: analysis of DNA restriction fragments and detection of single DNA molecules on microchips *Anal. Chem.* **69** 3451–7
[7] Ehrlich D J and Matsudaira P 1999 Microfluidic devices for DNA analysis *Trends Biotechnol.* **17** 315–19
[8] Paegel B M, Blazej R G and Mathies R A 2003 Microfluidic devices for DNA sequencing: sample preparation and electrophoretic analysis *Curr. Opin. Biotechnol.* **14** 42–50
[9] Ehrfeld W, Hessel V and Löwe H 2000 *Microreactors: New Technology for Modern Chemistry* (New York: Wiley) chapter 3
[10] Hessel V, Löwe H and Schönfeld F 2005 Micromixers—a review on passive and active mixing principles *Chem. Eng. J.* **107** 205–14
[11] Nguyen N-T and Wu Z 2005 Micromixers—a review *J. Micromech. Microeng.* **15** R1–16
[12] Hardt S, Drese K S, Hessel V and Schonfeld F 2005 Passive micromixers for applications in the microreactor and μTAS fields *Microfluid. Nanofluid.* **1** 108–18
[13] Mengeaud V, Josserand J and Girault H H 2002 Mixing processes in a zigzag microchannel: finite element simulations and optical study *Anal. Chem.* **74** 4279–86
[14] Chen J K and Yang R J 2007 Electroosmotic flow mixing in zigzag microchannels *Electrophoresis* **28** 975–83
[15] Liu R H, Stremler M A, Sharp K V, Olsen M G, Santiago J G, Adrian R J, Aref H and Beebe D J 2000 Passive mixing in a three-dimensional serpentine microchannel *J. Microelectromech. Syst.* **9** 190–98
[16] Vanka S P, Luo G and Winkler C M 2004 Numerical study of scalar mixing in curved channels at low Reynolds numbers *AIChE J.* **50** 2359–68
[17] Johnson T J, Ross D and Locascio L E 2002 Rapid microfluidic mixing *Anal. Chem.* **74** 45–51
[18] Stroock A D, Dertinger S K W, Adjari A, Mezic I, Stone H A and Whitesides G M 2002 Chaotic mixer for microchannels *Science* **295** 647–51
[19] Wang L, Yang J T and Lyu P C 2007 An overlapping crisscross micromixer *Chem. Eng. Sci.* **62** 711–20
[20] Gobby D, Angeli P and Gavriilidis A 2001 Mixing characteristics of T-type microfluidic mixers *J. Micromech. Microeng.* **11** 126–32
[21] Chung C K and Shih T R 2007 A rhombic micromixer with asymmetrical flow for enhancing mixing *J. Micromech. Microeng.* **17** 2495–504
[22] Chung C K and Shih T R 2008 Effect of geometry on fluid mixing of the rhombic micromixers *Microfluid. Nanofluid.* **4** 419–25
[23] Mouza A A, Patza C M and Schönfeld F 2008 Mixing performance of a chaotic micromixer *Chem. Eng. Res. Des.* **86** 1128–34
[24] 2006 CFX-11.0, Solver Theory, ANSYS
[25] Sinton D 2004 Microscale flow visualization *Microfluid. Nanofluid.* **1** 2–21
[26] Culbertson C T, Jacobson S C and Ramsey J M 1998 Dispersion sources for compact geometries on microchips *Anal. Chem.* **70** 3781–9
[27] Günthur A, Khan S A, Thalmann M, Thrachsel F and Jensen K F 2004 Transport and reaction in segmented gas–liquid flow *Lab Chip* **4** 278–86
[28] Kim D S, Lee S W, Kwon T H and Lee S S 2004 A barrier embedded chaotic micromixer *J. Micromech. Microeng.* **14** 798–805
[29] Schönfeld F and Hardt S 2004 Simulation of helical flows in microchannels *AIChE J.* **50** 771–8